Customized Reversible Stapling for Selective Delivery of Bioactive Peptides

Zizhen Zeng, Jibao Zhu, Xiaoyu Deng, Huanwen Chen, Yi Jin, Emeric Miclet, Valérie Alezra, Yang Wan

Customized Reversible Stapling for Selective Delivery of Bioactive Peptide

Zizhen Zeng,[#] Jibao Zhu, [#] Huanwen Chen, Yi Jin, Emeric Miclet, † Valérie Alezra, ‡ Yang Wan*

ABSTRACT: We have developed a new concept for reversible peptide stapling that involves a macrocyclization between two amino groups and a decyclization promoted via dual 1,4-elimination. Depending on the trigger moiety, this strategy could be employed to selectively deliver peptides to either intracellular or extracellular targets. As a proof of concept, a peptide inhibitor targeting the lysine-specific demethylase was temporarily cyclized to enhance its stability and ability to cross the cell membrane. Once inside the cells, the biologically active linear peptide was released under reducing environment. Moreover, we have developed reversibly stapled peptides using antimicrobial peptides (RStAMPs) whose bioactive helical conformation can be temporarily destabilized by stapling the peptide backbone. The resulting helix-distorted RStAMPs are non-toxic and highly resistant to protease hydrolysis while at the infection site, RStAMPs can be rapidly activated by the overproduced H2O2 through a dual 1,4-elimination. The latter restored the helical structure of the native peptide and its antimicrobial activity. This works illustrates a highly valuable macrocyclization strategy for the peptide community, and should greatly benefit the field of peptide delivery.

Peptides are biological macromolecules whose versatile functions are largely determined by their conformational structures. They are an important class of therapeutics with several advantages, including high potency and a broad range of targets, but their use is hampered by their poor *in vivo* stability,[1] low cell membrane penetration, and lack of specificity. Stapling (or macrocyclization) and polymer conjugation are two commonly used approaches for enhancing the pharmacological properties of peptide drugs.[2–7] Often, stapled or polymer-conjugated peptides have significantly enhanced metabolic stability. However, in some cases, polymer conjugation can mask the interaction site between the peptide and its target, or destabilize the bioactive conformation, in both cases resulting in a significant (or total) loss of peptide activity.[8–11] To take advantages of modified peptides while avoiding their loss of activity, many groups have developed approaches based on reversible modifications. The strategy is to temporarily mask the activity of peptide and restore it upon stimulation. In this context, reversible or degradable polymer conjugation of peptides has been extensively investigated, where the polymers are tethered to peptides via customized linkers and could be removed under various stimulis.[12–14] In comparison, reversible peptide stapling is under-exploited, although it is very promising as it avoids the use of polymers such as polyethylene glycol (PEG) that have shown potential hypersensitivity.[15]

It is understandable that the reversible polymerization is more chemically flexible, as the polymers can be removed by a single cleavage of the covalent bond, a way we call "one trigger, one release". In comparison, the traceless release of the peptide from the stapled state would theoretically require the cleavage of two covalent bonds at both sides of the staple, therefore requiring "two triggers, two releases" (see Scheme 1A). This severely restricts the chemical accessibility of stapled peptides and the efficiency of subsequent decyclization. To date, tethering between cysteine or methionine residues is the predominant approach to design reversibly stapled peptides, whose activity can be restored by reacting with intracellular abundant thiols (Scheme 1A).[16–21] While elegant, the activation

Scheme 1. (A) Schematic representation of reversibly stapled peptides activated by intracellular thiols. (B) Schematic representation of reversibly stapled peptides designed in this work. Our approach is designed to tolerate various triggers. Upon activation, stapled peptides will subsequently undergo dual 1,4-eliminations to release active peptides.

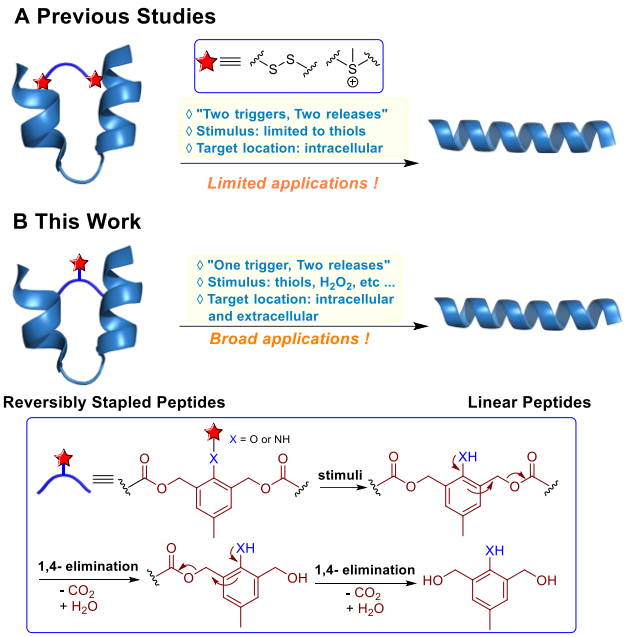

of reversibly stapled peptides of current approaches is exclusively relying on the intracellular thiols,[22] significantly limiting the potential of reversible stapling as a general approach for peptide delivery. Particularly, the available approaches are not suitable for extracellular peptides as antimicrobial peptides (AMPs) targeting cell membranes rather than intracellular receptors.[23] Thus, a simple and versatile reversible staple system that is compatible with various disease-associated stimulus should have great potential in the field of peptide delivery.

In this paper, we report an innovative strategy of reversible stapling that involves a new mechanism of decyclization. In our design, peptide stapling occurs between the widely prevalent amino groups by forming carbamate groups. Upon a single stimulation on the responsive moiety, the peptide staple could be removed via a spontaneous dual 1,4-eliminations, leading to a "one trigger, two releases" mechanism (Scheme 1B). Similar to reversible polymerization, this system is expected to be chemically tolerant to a large variety of

triggers,[24] and therefore could greatly expand the scope of potential applications. To demonstrate the broad range of applications, we decided in this work to prepare two linkers (**a** and **b**) that bear a thiol- and H_2O_2-sensitive moiety, respectively (Figure 1A). Linker **a** contains a disulfide bond that could be reduced by the high level of glutathione in the cells. The terminal azide group on linker **a** allows further modifications with other functional group. Linker **b** comprises an H2O2-sensitive boronic acid moiety. We chose it because H2O2 concentration is known to be elevated in many pathological conditions including (bacterial infection induced) inflammation,[25,26] and cancer.[26] Moreover, the extracellular concentration of H2O2 is considered much higher than its intracellular concentration.[25,26] In our design, reduction of the disulfide bond by glutathione or oxidation of the boronic acid in the presence of H_2O_2 will form a phenolate that will subsequently undergo spontaneous dual 1,4-eliminations, resulting in the release of linear peptides. Preparation of the removable linker **a** and protected linker **b** (Prot-**b**, as a pinacol boronic ester) are described in the supporting information (Scheme S1 and S2). The reactivity of linkers **a** and Prot-**b** towards various amino acids was screened. We found that they could both react with the amine groups (including the *N*-terminus and the lysine side chain), the thiol group of cysteine, and the imidazole group of histidine at 25 or 40 °C (Figure S1). Before attaching them to bioactive peptides, linkers **a** and **b** were linked to peptides that have two unprotected Lys positioned at i, i+4(**1**), i+6(**2**), i+8(**3**), and i+11(**4**, **5**), respectively. All coupling reactions were performed smoothly in solution conditions (10 mM in DMSO) with desired cyclic peptides obtained in satisfactory yield, as shown Figure 1B. Noteworthy, we used Prot-**b** to make the coupling reaction and the boronic ester was fully deprotected in the presence of catalytic trifluoroacetic acid and excess of methylboronic acid,[27] in order to increase the hydrophilicity of the stapled peptides. Next, we tested if linkers **a** and Prot-**b** were compatible with on-resin peptide cyclization. Based on our trials, cyclic peptides stapled with linker **a** directly onto the solid support were all successfully obtained in moderate yields. However, under the same conditions, cyclization of peptides with the protected linker **b** gave very low yields, probably because of the degradation of the boronic ester-containing peptides in the resin cleavage cocktail (TFA/TIS/H_2O).

Next, we used peptide **1a** and **1b** (Figure 1C) as examples to examine whether linear peptides could be regenerated from

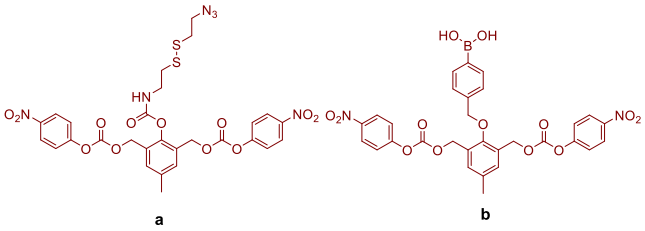

Peptide	Linker[a,b]	Stapled position
Ac-K_1RGDK_5A-NH2 (**1**)	**a**(30%), **b**(22%)	i, i+4
Ac-K_1VAGRTK_7A-NH2(**2**)	**a**(32%), **b**(25%)	i, i+6
Ac-K_1LALRLALK$_9$ALRAALRLA-NH2 (**3**)	**a**(28%), **b**(15%)	i, i+8
Ac-K_1LALRLALRALK$_{12}$AALRLA-NH2 (**4**)	**a**(25%), **b**(18%)	i, i+11
Ac-RLALK$_5$LALRALRAALK$_{16}$LA-NH2 (**5**)	**a**(28%), **b**(20%)	i, i+11

a. Stapling conditions in solution: peptide (1.0 equiv., 10 mM), linker (1.2 equiv.), DiEA(10 equiv.), DMSO, 25 °C. Additional step for linker **b**: Methylboronic acid (10 equiv), 5% TFA/DCM, RT, 2 h. *b*. purified yield by HPLC, 2 steps for linker **b**.

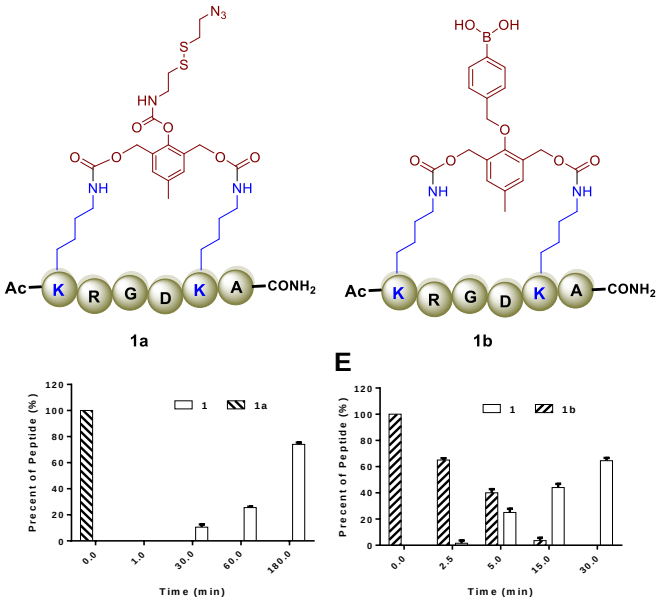

Figure 1. (A) Thiols- (**a**) and H2O2-responsive (**b**) linkers synthesized in this work. (B) Different peptide sequences and ring sizes. The lysines that have been linked are labelled by their number in the peptide sequence (C) Structures of stapled peptides **1a** and **1b**. Regeneration (%) of peptide **1** from cyclized peptides (200 μM) in the presence of 1 mM TCEP (D) or H_2O_2 (E) in PBS (pH 7.4) at 37 °C. Peptide quantifications were monitored by reverse-phase HPLC.

the macrocycles upon stimulation. We found that upon treatment with tris(2-carboxyethyl)phosphine (TCEP, 5 equiv., 1mM) in PBS buffer (pH 7.4), peptide **1a** showed time-dependent regeneration of the parental peptide **1** (Figure 1D). The proposed reaction mechanism of peptide **1a** in a reducing environment is shown in Figure S2. In the presence of TCEP, the disulfide bond is immediately cleaved (complete disappearance of the peptide **1a** after one minute on Figure 1D) to form linear intermediate **S9**, and the resulting thiol react intramolecularly to form a thiazolidinone. After a dual 1,4-elimination, the unmodified linear peptide **1** is formed. Next, we examined whether the activation of peptide **1b** occurred in a H_2O_2-specific manner. As shown in Figure 1E, upon treatment with 1 mM H_2O_2, the initial concentration of 200 μM of **1b** decreased dramatically and was traceless after 15 min. Meanwhile, the linear peptide **1** was rapidly regenerated to more than 60% of the precursor concentration within 30 min. The formation of an intermediate and byproducts was also identified, as can be seen in Figure S3. Further, gradual addition of H_2O_2 up to 10 equiv. to a solution of **1b** was investigated. As expected, by increasing the amount of H_2O_2, greater percentage of decomposed **1b** was observed along with a larger quantity of released linear precursor (Figure S4). Taken together, these observations indicate that the stapled peptide **1b** was readily processed by H_2O_2 to release peptide **1**. We then assessed the reactivity specificity of our boronic acid motif using other biologically relevant extracellular reactive oxygen species (ROS). For this, **1b** (200 μM) was incubated with various ROS (500 μM) for 1 h. Compared to H_2O_2, which fully consumed the stapled peptide, other ROS, or H_2O_2 in the presence of catalase, showed little to no effect on peptide **1b**, highlighting specific disassociation of **1b** by H_2O_2 (Figure S5).

Encouraged by the results obtained on model peptides, we next investigated whether this strategy could be used for the selective delivery of functional peptides. Interfering peptides targeting protein-protein interactions (PPIs) are promising anticancer drugs, but their practical application is hampered by insufficient permeability

to cell-membrane.[28] Considering that macrocyclization is one of the frequently adopted approaches to improve the cellular uptake of peptides,[2,29] we wondered whether the reversible stapling presented in this work could confer increased cell-membrane permeability to cyclic peptides and thus allow selective activation under intracellular reducing conditions. As a proof of concept, we synthesized three cyclic analogues of peptides **6** (Figure 2A), a LSD1-specific inhibitor derived from the SNAIL1 peptide.[20] Peptide **7** was synthesized by coupling the amino groups of the *N*-terminal proline and the lysine side chain with the linker **a** on solid support. In order to further increase the selectivity towards cancer cells, an extra biotin moiety was tethered to **7** via Cu-catalyzed azide-alkyne cycloaddition to afford peptide **8**.[30] Peptide **9** serves as a non-cleavable control. First, we tested if the linear peptide could be released from the macrocycle. As for peptide **1a**, peptide **8** was rapidly consumed to regenerate linear precursors in the presence of TECP in 30 min (Figure S6). Then we examined the K_i values for LSD1 inhibition, which were measured in the peroxidase-coupled reaction assay and fitted with steady-state kinetics.[31] As summarized in Figure 2B, linear peptide **6** has the most potent LSD1 inhibitory activity. As expected, all cyclic peptides exhibited about 16- to 36-fold weaker activity than the parent peptide, which is in agreement with previous works.[20] To assess the biological activity of the designed cyclic peptides, we evaluated their growth-inhibitory effects on 4T1 breast cancer cells, whose growth is highly sensitive to LSD1 inhibition.[32] As can be seen in Figure 2C, although the cyclic peptides had much higher K_i values, they all exhibited stronger growth-inhibitory activity against 4T1 cells than the linear peptide **6**, strongly suggesting the increased membrane permeability of macrocycles. Compared to non-cleavable peptide **9**, peptide **7** showed an equal K_i value but slightly stronger inhibition of cell growth,

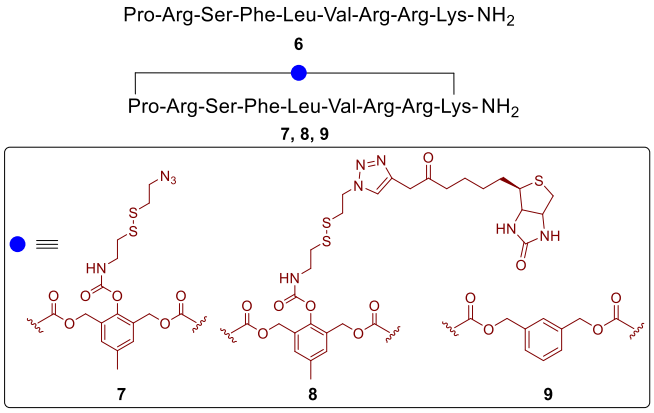

Peptide	K_i (μM)
6	0.0091 ± 0.0034
7	0.28 ± 0.014
8	0.15 ± 0.023
9	0.33± 0.01

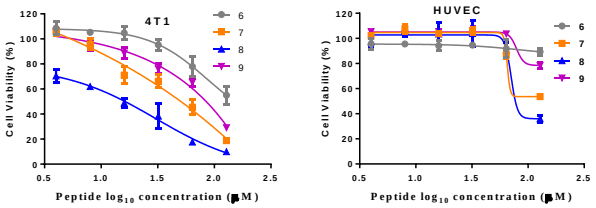

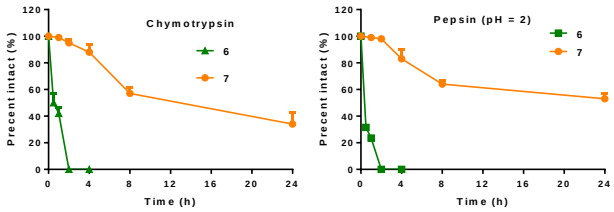

Figure 2. (A) Peptide sequence of peptide **6** and its cyclic derivatives. (B) K_i values of projected peptides for LSD1 inhibition. (C) Cytotoxicity of linear and cyclic peptides towards 4T1 and HUVEC cells. (D) *In vitro* chymotrypsin (0.25 μg/mL) and pepsin (pH = 2) digestion assay. Peptides (200 μM) incubated for different time intervals.

presumably due to the intracellular release of the linear peptide **6** which is more potent towards LSD1 than the cyclic peptide **9**. Among all candidates, peptide **8** has the most potent cell activity (IC50~ 10 μM), largely owing to the additional binding affinity between biotin and vitamin receptors that are overproduced in 4T1 cancer cells. By comparison, all peptides showed a very weak growth-inhibitory effect on normal human cell HUVEC, reflecting the fact that LSD1 is a highly selective target on cancer cells compared to normal cells.

Stapled peptides are known to have an improved proteolytic stability. To demonstrate this property, we compared the stability of peptides **6** and **7** by incubation with chymotrypsin and pepsin. As reported in Figure 2D, stapled peptides showed a much higher protease stability than the linear precursor. While **6** was completely degraded within 2 h for both proteases, a large amount of peptide **7** remained intact after 24 h of incubation. In conclusion, compared with linear peptide **6**, reversible stapled peptides possess greater proteolytic stability as well as higher membrane permeability, leading to superior activity against cancer cells.

To further demonstrate potential biological applications, we next investigated the possibility of reversible stapling mediated by dual 1,4-elimination on selective delivery of antimicrobial peptides. We chose AMPs considering that they represent one of the most promising alternatives to antibiotics, in the era of increasing bacterial resistance. Owing to their unique antibacterial mechanism consisting mainly in the lysis of cell membranes, AMPs rarely cause bacterial resistance.[33] However, the application of AMPs is severely hampered by their poor metabolic stability and non-specific toxicity against mammalian cells, which is largely associated with their secondary structure.[34,35] Although irreversible stapling has been widely used to stabilize helical conformations, peptides constrained with additional tethers at undesired positions were found to have distorted or altered secondary structures, resulting in a significant loss of both activity and toxicity. [10,11,36–39] We thereby envisioned that reversible stapling could be used to design reversibly stapled AMPs (RStAMPs) with switchable conformational properties. Interestingly, their membrane-activity could be restored by selective removal of the staple at the target. Temporin L (TL, **10**), the most active AMP in the temporin family,[40] was used to establish our approach based on reversible stapling. Cyclization of the temporin L were performed by tethering its *N*-terminus and lysine side chain with linker **1b** in solution phase. To compare stapled TL analogues of different ring sizes, we prepared peptide **11**, a mutant of TL with lysine and arginine exchanged (Figure 3A). The regeneration of linear AMPs was subsequently preformed upon treatment with H_2O_2. As shown in Figure S7, the HPLC analysis proved that both stapled peptides (100 μM) were completely consumed to regenerate linear precursors in the presence of H_2O_2 (500 μM) in 1 h. To explore the conformational behavior of stapled peptides and corresponding linear precursors, we performed a circular dichroism

(CD) study of these peptides in both aqueous solution and SDS micelles, a rough model of biological membranes. Both peptide **10** and **11** showed a disordered structure in water (Figure S8) while they adopted a typical helical conformation in SDS micelles, as indicated by two minima of ellipticity near 207 and 222 nm (Figure 3B). The CD spectrum of RStAMP **13** in water displayed a slight helical character, probably due to the restricted flexibility imposed by the cyclization. However, the content of helix of both stapled peptides **12** (18.1%)and **13** (25.2%)was significantly reduced compared to the linear peptides (64.9% & 55.5%)in SDS micelles, suggesting that the canonical helical conformation was not compatible with stapling. Upon addition of H_2O_2, the content of helical conformations (54.0% & 45.3%) in SDS micelles increased dramatically approaching that of reference linear peptides (Figure 3B). In contrast to helix stabilization, which requires staples to be positioned on specific residues, it is interesting to note that equivalent helix distortions can be obtained with many staple positions, as evidenced by the similar CD spectra obtained for **12** and **13**. This should greatly expand the potential field of applications of this strategy. We then measured the membrane-disruptive activity of stapled peptides and their linear precursors by incubating them with calcein-encapsulated liposome (DOPE/DOPG,

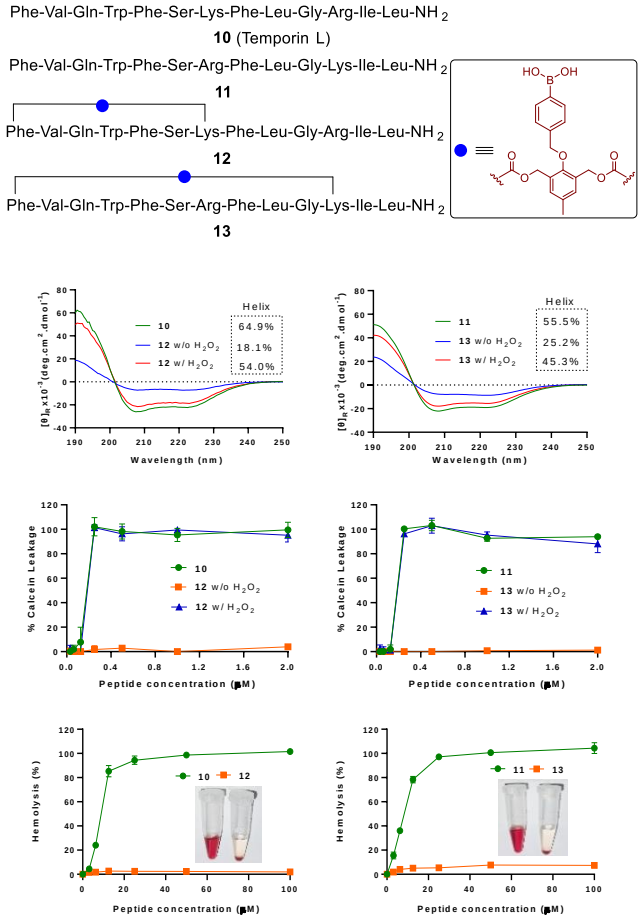

Figure 3. (A) Peptide sequences of linear and cyclic antimicrobial peptides presented in this work. (B) CD Spectra and the content of helix of peptides at 100 μM in SDS micelles (20 mM). The concentration of H2O2, when present, was 500 μM. (C) Percentage of calcein leakage from negatively charged liposomes after incubation with **11** and **13** (with or without H_2O_2, 100 μM) at various concentrations for 1 h. (D) The hemolytic activity of stapled peptides and their corresponding linear precursors. 'w/' - 'with', 'w/o' - 'without'. Inset: hemolysis of corresponding peptide at 1oo μM.

75/25, w/w), a widely used model system to simulate negatively charged bacterial cell membranes.[41] As it is demonstrated in Figure 3C, both **10** and **11** induced a progressive increase of calcein leakage with concentration above 0.25 μM (peptide/lipid, 1/2000, molar ratio). On the other hand, stapled peptides **12** and **13** caused almost no calcein leakage at concentrations up to 2 μM. However, upon treatment with H_2O_2, the calcein leakage significantly increased to the same level as their helical precursors, demonstrating that restoration of the helical conformation contributed to the recovery of membrane activity. Next, we carried out biological assays using the two stapled peptides or their linear precursors. As shown in Figure 3D, both **10** and **11** induced hemolysis at very low concentrations, which is in agreement with literature.[42] Since the hemolytic activity of AMPs is highly dependent on their secondary structure, as established by the correlation between the helical content and the lytic propensity of antimicrobial peptides,[43–51] the reduction in hemolysis observed with stapled peptides is directly related to their distorted helical conformation. Non-toxicity to mammalian cells is also important for the clinical application of AMPs. Therefore, we performed CCK-8 assays on LO2 (Human Normal Liver Cells) and HUVEC (Human Umbilical Vein Endothelial Cells) (Figure S9). These assays demonstrated that the stapled peptides exhibited much lower cytotoxicity than their corresponding helical precursors, again due to the disrupted helical structure.

Then, we wondered if the helix-distorted RStAMPs can be activated to restore their antibacterial activity at the infection site. For this, we intended to measure the MICs of three *S. aureus* strains (MRSA, ATCC 25923, and ATCC 29213), noting that MRSA is one of the most threatening drug-resistant bacteria.[52] Prior to the measurement, we tested the sensitivity of the strains towards addition of H_2O_2. We found that, in the range of 25-200 μM, H_2O_2 showed little to no effect on bacterial growth (Figure S10), which is in line with previous research.[53] Hence, measuring MICs in the presence of 100 μM H_2O_2 could reasonably simulate the microenvironment of bacterial infection without inhibiting bacterial growth. As shown in Table 1, both **10** and **11** exhibited potent activities against all bacterial strains. It is noteworthy that the mutation of arginine to lysine induced no decrease of activity (even a slight improvement). Not surprisingly, RStAMPs barely inhibited bacterial growth. However, their bactericidal activity was restored to the same level as linear peptides in the presence of H_2O_2, highlighting their great potential in the treatment of bacterial infection. To visually examine the recovered membrane-disruptive activity of peptides upon treatment with H_2O_2, scanning electron microscope (SEM) experiments were performed by treating MRSA with different peptides. Upon exposure to **10** or **11** (2× MIC), the cell membrane of MRSA was impaired to the point that cell contents leaked out (Figure 4 and S11). No disruption on the integrity of cell membrane was found for cells treated with stapled peptides. By comparison, significantly damaged MRSA cells were observed upon treatment with stapled peptide in the presence of H_2O_2. To summarize, the toxicity against normal mammalian cells of helix-distorted RStAMPs is low compared to their linear precursors while their secondary structure and antibacterial activity can be rapidly restored upon activation by H_2O_2

Table 1. The antibacterial activity of linear peptides and stapled peptides (with or without H_2O_2) against *S. aureus* strains (MRSA, ATCC 25923, and ATCC 29213).

Peptides	MIC (μM) [a]		
	MRSA	ATCC 25923	ATCC 29213
10	4	4	4
10 w/ H_2O_2 [b]	4	4	4
12 w/o H_2O_2	>32	>32	>32

12 w/ H_2O_2	6	6	6
11	2	2	2
11 w/ H_2O_2	2	2	2
13 w/o H_2O_2	>32	>32	>32
13 w/ H_2O_2	3	3	3

[a] 32 μM was the maximal tested concentration; [b] The concentration of H_2O_2 was 100 μM.

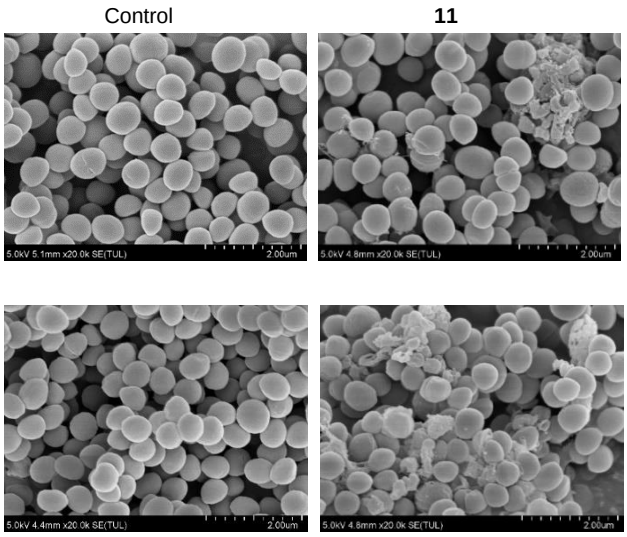

Figure 4. SEM photographs of MRSA cells treated with peptide **11** or **13** (with or without H_2O_2, 100 μM) at their 2x MIC for 1 h.

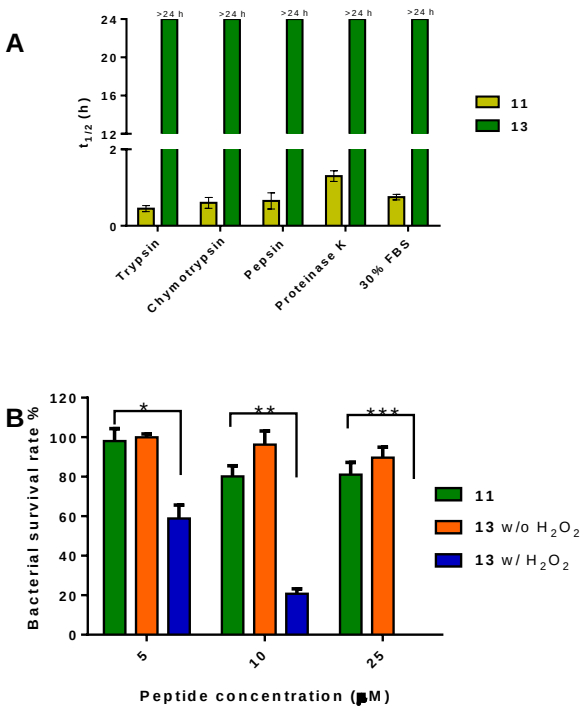

Figure 5. (A) *In vitro* half-life (t1/2) of peptide **11** and **13** towards protease and serum (30% FBS) digestion. Protease concentrations: trypsin (0.25 μg/mL), chymotrypsin (0.1 μg/mL), pepsin (10 μg/mL, pH = 2), proteinase K (0.05 μg/mL). (B) The survival rate of MRSA incubated with peptides which were pretreated by trypsin (0.25 μg/mL) for 1 h. **P* < 0.05, ***P* < 0.01, ****P* < 0.001.

The ability to withstand enzymatic degradation in the circulatory system is an important requirement for any potential peptide drug. Therefore, we next evaluated the susceptibility of RStAMP **13** to proteolytic cleavage. As shown in Figure 5A and S12, in each conditions, more than 50% of peptide **13** remained intact after 24 h incubation while linear peptide **11** was totally digested within 2 to 4 hours, with half time around 0.4~1.3 h. A similar tendency was observed when peptides were treated with 30% fetal bovine serum. To demonstrate the advantage of peptides with high protease stability, we measured the MRSA survival rate after incubation with **11** or **13** which were pretreated by trypsin for 1 h. It could be seen that **11** largely lost its antimicrobial activity after incubation with trypsin (Figure 5B). Peptide **13** showed no antibacterial activity but impressively, upon addition of H_2O_2 (100 μM), bacteria were efficiently killed and totally eliminated. This substantiates that peptide **13** is highly resistant to proteolytic hydrolysis and demonstrates a great potential in the treatment of bacterial infection *in vivo*, at 25 μM.

In summary, we validated a new concept of reversible peptide stapling where the parent peptide could be regenerated, in a traceless manner and upon a single stimulation of a trigger group via dual 1,4-elimination. Significantly, this strategy could be used to deliver peptides directed to both intracellular and extracellular targets, depending on the trigger moiety. We showed that reversibly stapled peptides exhibited stronger cytotoxicity than linear peptides, due to enhanced membrane permeability and the subsequent release of linear peptides under reducing environment. We have also synthesized a pair of RStAMPs derived from temporin L, a known helical AMP that exhibits potent activity while unfortunately also displays high toxicity towards mammalian cells. The resulting RStAMPs are conformationally distorted, non-toxic, highly stable, and can be selectively activated by H_2O_2 via dual 1,4-elimination, leading to a fully restored antibacterial activity. Taken together, the proposed reversible stapling strategy should be combinable with various trigger groups and could be applied to many other peptides of therapeutic interest, developed for drug delivery or designed for biomaterials applications.

ASSOCIATED CONTENT

Supporting Information

Supporting Information. This material is available free of charge via the Internet at http://pubs.acs.org." Experimental details, NMR spectra, supplementary figures (pdf).

AUTHOR INFORMATION

Corresponding Author

yang.wan89@outlook.com *orcid.org/0000-0003-3842-5074.*

Present Addresses

† Sorbonne Université, Ecole Normale Supérieure, PSL University, CNRS, Laboratoire des Biomolécules, 4 place Jussieu, 75252 Paris Cedex 05, France.

‡ Laboratoire de Méthodologie, Synthèse et Molécules Thérapeutiques, ICMMO, Université Paris-Saclay, Orsay 91400, France.

Author Contributions

‡ Z. Z. and J. Z. contributed equally to this work.

Notes

The authors declare no competing financial interests.

ACKNOWLEDGMENT

This work was financially supported by the National Natural Science Foundation of China (No. 21967012) and Jiangxi Provincial Natural Science Foundation (No. 20202ACBL216016; 20212ACB206007). Y. W. also acknowledge the support from Jiangxi University of Chinese Medicine Science and Technology Innovation Team Development Program.

REFERENCES

(1) Fosgerau, K.; Hoffmann, T. Peptide Therapeutics: Current Status and Future Directions. *Drug Discov. Today* **2015**, *20* (1), 122–128.

(2) Li, X.; Chen, S.; Zhang, W.-D.; Hu, H.-G. Stapled Helical Peptides Bearing Different Anchoring Residues. *Chem. Rev.* **2020**, *120* (18), 10079–10144.

(3) Jwad, R.; Weissberger, D.; Hunter, L. Strategies for Fine-Tuning the Conformations of Cyclic Peptides. *Chem. Rev.* **2020**, *120* (17), 9743–9789.

(4) Jing, X.; Jin, K. A Gold Mine for Drug Discovery: Strategies to Develop Cyclic Peptides into Therapies. *Med. Res. Rev.* **2020**, *40* (2), 753–810.

(5) Ko, J. H.; Maynard, H. D. A Guide to Maximizing the Therapeutic Potential of Protein–Polymer Conjugates by Rational Design. *Chem. Soc. Rev.* **2018**, *47*(24), 8998-9014.

(6) Pasut, G.; Veronese, F. M. State of the Art in PEGylation: The Great Versatility Achieved after Forty Years of Research. *J. Controlled Release* **2012**, *161* (2), 461–472.

(7) Pelegri-O'Day, E. M.; Lin, E.-W.; Maynard, H. D. Therapeutic Protein–Polymer Conjugates: Advancing Beyond PEGylation. *J. Am. Chem. Soc.* **2014**, *136* (41), 14323–14332.

(8) Imura, Y.; Nishida, M.; Ogawa, Y.; Takakura, Y.; Matsuzaki, K. Action Mechanism of Tachyplesin I and Effects of PEGylation. *Biochim. Biophys. Acta BBA - Biomembr.* **2007**, *1768* (5), 1160–1169.

(9) Mizejewski, G. J.; Muehlemann, M.; Dauphinee, M. Update of Alpha Fetoprotein Growth-Inhibitory Peptides as Biotherapeutic Agents for Tumor Growth and Metastasis. *Chemotherapy* **2006**, *52* (2), 83–90.

(10) Stone, T. A.; Cole, G. B.; Nguyen, H. Q.; Sharpe, S.; Deber, C. M. Influence of Hydrocarbon-Stapling on Membrane Interactions of Synthetic Antimicrobial Peptides. *Bioorg. Med. Chem.* **2018**, *26* (6), 1189–1196.

(11) Hirano, M.; Saito, C.; Goto, C.; Yokoo, H.; Kawano, R.; Misawa, T.; Demizu, Y. Rational Design of Helix-Stabilized Antimicrobial Peptide Foldamers Containing α, α-Disubstituted Amino Acids or Side-Chain Stapling. *ChemPlusChem* **2020**, *85* (12), 2731–2736.

(12) Filpula, D.; Zhao, H. Releasable PEGylation of Proteins with Customized Linkers. *Adv. Drug Deliv. Rev.* **2008**, *60* (1), 29–49.

(13) Gong, Y.; Leroux, J.-C.; Gauthier, M. A. Releasable Conjugation of Polymers to Proteins. *Bioconjug. Chem.* **2015**, *26* (7), 1172–1181.

(14) Rose, D. A.; Treacy, J. W.; Yang, Z. J.; Ko, J. H.; Houk, K. N.; Maynard, H. D. Self-Immolative Hydroxybenzylamine Linkers for Traceless Protein Modification. *J. Am. Chem. Soc.* **2022**, *144* (13), 6050–6058.

(15) Shah, S.; Prematta, T.; Adkinson, N. F.; Ishmael, F. T. Hypersensitivity to Polyethylene Glycols: The Journal of Clinical Pharmacology. *J. Clin. Pharmacol.* **2013**, *53* (3), 352–355.

(16) Qian, Z.; Rhodes, C. A.; McCroskey, L. C.; Wen, J.; Appiah-Kubi, G.; Wang, D. J.; Guttridge, D. C.; Pei, D. Enhancing the Cell Permeability and Metabolic Stability of Peptidyl Drugs by Reversible Bicyclization. *Angew. Chem. Int. Ed.* **2017**, *56* (6), 1525–1529.

(17) Qian, Z.; Xu, X.; Amacher, J. F.; Madden, D. R.; Cormet-Boyaka, E.; Pei, D. Intracellular Delivery of Peptidyl Ligands by Reversible Cyclization: Discovery of a PDZ Domain Inhibitor That Rescues CFTR Activity. *Angew. Chem. Int. Ed.* **2015**, *54* (20), 5874–5878.

(18) Grison, C. M.; Burslem, G. M.; Miles, J. A.; Pilsl, L. K. A.; Yeo, D. J.; Imani, Z.; Warriner, S. L.; Webb, M. E.; Wilson, A. J. Double Quick, Double Click Reversible Peptide "Stapling." *Chem. Sci.* **2017**, *8* (7), 5166–5171.

(19) Shi, X.; Zhao, R.; Jiang, Y.; Zhao, H.; Tian, Y.; Jiang, Y.; Li, J.; Qin, W.; Yin, F.; Li, Z. Reversible Stapling of Unprotected Peptides via Chemoselective Methionine Bis-Alkylation/Dealkylation. *Chem. Sci.* **2018**, *9* (12), 3227–3232.

(20) Kitagawa, H.; Kikuchi, M.; Sato, S.; Watanabe, H.; Umezawa, N.; Kato, M.; Hisamatsu, Y.; Umehara, T.; Higuchi, T. Structure-Based Identification of Potent Lysine-Specific Demethylase 1 Inhibitor Peptides and Temporary Cyclization to Enhance Proteolytic Stability and Cell Growth-Inhibitory Activity. *J. Med. Chem.* **2021**, *64*(7), 3707−3719.

(21) Amano, Y.; Umezawa, N.; Sato, S.; Watanabe, H.; Umehara, T.; Higuchi, T. Activation of Lysine-Specific Demethylase 1 Inhibitor Peptide by Redox-Controlled Cleavage of a Traceless Linker. *Bioorg. Med. Chem.* **2017**, *25* (3), 1227–1234.

(22) Schafer, F. Q.; Buettner, G. R. Redox Environment of the Cell as Viewed through the Redox State of the Glutathione Disulfide/Glutathione Couple. *Free Radic. Biol. Med.* **2001**, *30* (11), 1191–1212.

(23) Zasloff, M. Antimicrobial Peptides of Multicellular Organisms. *Nature* **2002**, *415* (6870), 389–395.

(24) Lee, M. H.; Sharma, A.; Chang, M. J.; Lee, J.; Son, S.; Sessler, J. L.; Kang, C.; Kim, J. S. Fluorogenic Reaction-Based Prodrug Conjugates as Targeted Cancer Theranostics. *Chem. Soc. Rev.* **2018**, *47* (1), 28–52.

(25) Erttmann, S. F.; Gekara, N. O. Hydrogen Peroxide Release by Bacteria Suppresses Inflammasome-Dependent Innate Immunity. *Nat. Commun.* **2019**, *10* (1), 3493.

(26) Weinstain, R.; Savariar, E. N.; Felsen, C. N.; Tsien, R. Y. In Vivo Targeting of Hydrogen Peroxide by Activatable Cell-Penetrating Peptides. *J. Am. Chem. Soc.* **2014**, *136* (3), 874–877.

(27) Hinkes, S. P. A.; Klein, C. D. P. Virtues of Volatility: A Facile Transesterification Approach to Boronic Acids. *Org. Lett.* **2019**, *21* (9), 3048–3052.

(28) Bruzzoni-Giovanelli, H.; Alezra, V.; Wolff, N.; Dong, C.-Z.; Tuffery, P.; Rebollo, A. Interfering Peptides Targeting Protein–Protein Interactions: The next Generation of Drugs? *Drug Discov. Today* **2018**, *23* (2), 272–285.

(29) Bhardwaj, G.; O'Connor, J.; Rettie, S.; Huang, Y.-H.; Ramelot, T. A.; Mulligan, V. K.; Alpkilic, G. G.; Palmer, J.; Bera, A. K.; Bick, M. J.; Di Piazza, M.; Li, X.; Hosseinzadeh, P.; Craven, T. W.; Tejero, R.; Lauko, A.; Choi, R.; Glynn, C.; Dong, L.; Griffin, R.; van Voorhis, W. C.; Rodriguez, J.; Stewart, L.; Montelione, G. T.; Craik, D.; Baker, D. Accurate de Novo Design of Membrane-Traversing Macrocycles. *Cell* **2022**, 185(19), 3520-3532.e26.

(30) Russell-Jones, G.; McTavish, K.; McEwan, J.; Rice, J.; Nowotnik, D. Vitamin-Mediated Targeting as a Potential Mechanism to Increase Drug Uptake by Tumours. *J. Inorg. Biochem.* **2004**, *98* (10), 1625–1633.

(31) Mimasu, S.; Umezawa, N.; Sato, S.; Higuchi, T.; Umehara, T.; Yokoyama, S. Structurally Designed *Trans* -2-Phenylcyclopropylamine Derivatives Potently Inhibit Histone Demethylase LSD1/KDM1. *Biochemistry* **2010**, *49* (30), 6494–6503.

(32) Boulding, T.; McCuaig, R. D.; Tan, A.; Hardy, K.; Wu, F.; Dunn, J.; Kalimutho, M.; Sutton, C. R.; Forwood, J. K.; Bert, A. G.; Goodall, G. J.; Malik, L.; Yip, D.; Dahlstrom, J. E.; Zafar, A.; Khanna, K. K.; Rao, S. LSD1 Activation Promotes Inducible EMT Programs and Modulates the Tumour Microenvironment in Breast Cancer. *Sci. Rep.* **2018**, *8* (1), 73.

(33) Magana, M.; Pushpanathan, M.; Santos, A. L.; Leanse, L.; Fernandez, M.; Ioannidis, A.; Giulianotti, M. A.; Apidianakis, Y.; Bradfute, S.; Ferguson, A. L.; Cherkasov, A.; Seleem, M. N.; Pinilla, C.; de la Fuente-Nunez, C.; Lazaridis, T.; Dai, T.; Houghten, R. A.; Hancock, R. E. W.; Tegos, G. P. The Value of Antimicrobial Peptides in the Age of Resistance. *Lancet Infect. Dis.* **2020**, *20* (9), e216–e230.

(34) Jiang, Y.; Chen, Y.; Song, Z.; Tan, Z.; Cheng, J. Recent Advances in Design of Antimicrobial Peptides and Polypeptides toward Clinical Translation. *Adv. Drug Deliv. Rev.* **2021**, *170*, 261–280.

(35) Zeng, Z.-Z.; Huang, S.-H.; Alezra, V.; Wan, Y. Antimicrobial Peptides: Triumphs and Challenges. *Future Med. Chem.* **2021**, fmc-2021-0134.

(36) Klein, M. J.; Schmidt, S.; Wadhwani, P.; Bürck, J.; Reichert, J.; Afonin, S.; Berditsch, M.; Schober, T.; Brock, R.; Kansy, M.; Ulrich, A. S. Lactam-Stapled Cell-Penetrating Peptides: Cell Uptake and Membrane Binding Properties. *J. Med. Chem.* **2017**, *60* (19), 8071–8082.

(37) Bellavita, R.; Casciaro, B.; Di Maro, S.; Brancaccio, D.; Carotenuto, A.; Falanga, A.; Cappiello, F.; Buommino, E.; Galdiero, S.; Novellino, E.; Grossmann, T. N.; Mangoni, M. L.; Merlino, F.; Grieco, P. First-in-Class Cyclic Temporin L Analogue: Design, Synthesis, and Antimicrobial Assessment. *J. Med. Chem.* **2021**, *64* (15), 11675–11694.

(38) Etayash, H.; Pletzer, D.; Kumar, P.; Straus, S. K.; Hancock, R. E. W. Cyclic Derivative of Host-Defense Peptide IDR-1018 Improves Proteolytic Stability, Suppresses Inflammation, and Enhances In Vivo Activity. *J. Med. Chem.* **2020**, *63* (17), 9228–9236.

(39) Liu, B.; Zhang, W.; Gou, S.; Huang, H.; Yao, J.; Yang, Z.; Liu, H.; Zhong, C.; Liu, B.; Ni, J.; Wang, R. Intramolecular Cyclization of the Antimicrobial Peptide Polybia-MPI with Triazole Stapling: Influence on Stability and Bioactivity: Cyclization of the Polybia-MPI with Triazole Stapling. *J. Pept. Sci.* **2017**, *23* (11), 824–832.

(40) Romero, S. M.; Cardillo, A. B.; Ceron, M. C. M.; Camperi, S. A.; Giudicessi, S. L. Temporins: An Approach of Potential Pharmaceutic Candidates. *Surg. Infect.* **2020**, *21*(4), 309-322.

(41) Strömstedt, A. A.; Ringstad, L.; Schmidtchen, A.; Malmsten, M. Interaction between Amphiphilic Peptides and Phospholipid Membranes. *Curr. Opin. Colloid Interface Sci.* **2010**, *15* (6), 467–478.

(42) Carotenuto, A.; Malfi, S.; Saviello, M. R.; Campiglia, P.; Gomez-Monterrey, I.; Mangoni, M. L.; Gaddi, L. M. H.; Novellino, E.; Grieco, P. A Different Molecular Mechanism Underlying Antimicrobial and Hemolytic Actions of Temporins A and L. *J. Med. Chem.* **2008**, *51* (8), 2354–2362.

(43) Babii, O.; Afonin, S.; Berditsch, M.; Reisser, S.; Mykhailiuk, P. K.; Kubyshkin, V. S.; Steinbrecher, T.; Ulrich, A. S.; Komarov, I. V. Controlling Biological Activity with Light: Diarylethene- Containing Cyclic Peptidomimetics. *Angew. Chem.-Int. Ed.* **2014**, *53* (13), 3392–3395.

(44) Babii, O.; Afonin, S.; Garmanchuk, L. V.; Nikulina, V. V.; Nikolaienko, T. V.; Storozhuk, O. V.; Shelest, D. V.; Dasyukevich, O. I.; Ostapchenko, L. I.; Iurchenko, V.; Zozulya, S.; Ulrich, A. S.; Komarov, I. V. Direct Photocontrol of Peptidomimetics: An Alternative to Oxygen-Dependent Photodynamic Cancer Therapy. *Angew. Chem. Int. Ed.* **2016**, *55* (18), 5493–5496.

(45) Yeoh, Y. Q.; Yu, J.; Polyak, S. W.; Horsley, J. R.; Abell, A. D. Photopharmacological Control of Cyclic Antimicrobial Peptides. *ChemBioChem* **2018**, *19* (24), 2591–2597.

(46) Xiong, M.; Bao, Y.; Xu, X.; Wang, H.; Han, Z.; Wang, Z.; Liu, Y.; Huang, S.; Song, Z.; Chen, J.; Peek, R. M.; Yin, L.; Chen, L.-F.; Cheng, J. Selective Killing of Helicobacter Pylori with pH-Responsive Helix–Coil Conformation Transitionable Antimicrobial Polypeptides. *Proc. Natl. Acad. Sci.* **2017**, *114* (48), 12675–12680.

(47) Xiong, M.; Han, Z.; Song, Z.; Yu, J.; Ying, H.; Yin, L.; Cheng, J. Bacteria-Assisted Activation of Antimicrobial Polypeptides by a Random-Coil to Helix Transition. *Angew. Chem. Int. Ed.* **2017**, *56* (36), 10826–10829.

(48) Fan, Y.; Li, X.-D.; He, P.-P.; Hu, X.-X.; Zhang, K.; Fan, J.-Q.; Yang, P.-P.; Zheng, H.-Y.; Tian, W.; Chen, Z.-M.; Ji, L.; Wang, H.; Wang, L. A Biomimetic Peptide Recognizes and Traps Bacteria in Vivo as Human Defensin-6. *Sci. Adv.* **2020**, *6* (19), eaaz4767.

(49) Shi, J.; Fichman, G.; Schneider, J. P. Enzymatic Control of the Conformational Landscape of Self-Assembling Peptides. *Angew. Chem. Int. Ed.* **2018**, *57* (35), 11188–11192.

(50) Miller, S. E.; Tsuji, K.; Abrams, R. P. M.; Burke, T. R.; Schneider, J. P. Uncoupling the Folding-Function Paradigm of Lytic Peptides to Deliver Impermeable Inhibitors of Intracellular Protein–Protein Interactions. *J. Am. Chem. Soc.* **2020**, *142* (47), 19950–19955.

(51) Feng, Z.; Wang, H.; Wang, S.; Zhang, Q.; Zhang, X.; Rodal, A. A.; Xu, B. Enzymatic Assemblies Disrupt the Membrane and Target Endoplasmic Reticulum for Selective Cancer Cell Death. *J. Am. Chem. Soc.* **2018**, *140* (30), 9566–9573.

(52) Boucher, H. W.; Talbot, G. H.; Bradley, J. S.; Edwards, J. E.; Gilbert, D.; Rice, L. B.; Scheld, M.; Spellberg, B.; Bartlett, J. Bad Bugs, No Drugs: No ESKAPE! An Update from the Infectious Diseases Society of America. *Clin. Infect. Dis.* **2009**, *48* (1), 1–12.

(53) Fichman, G.; Andrews, C.; Patel, N. L.; Schneider, J. P. Antibacterial Gel Coatings Inspired by the Cryptic Function of a Mussel Byssal Peptide. *Adv. Mater.* **2021**, *33* (40), 2103677.